The Design and Development of a Low SWaP Communications System for a 1P Cube Satellite

Joseph Harounian, Patrick Blanchard, Trout Marnell, Saurav Basnet
Program of Electrical and Computer Engineering
Wentworth Institute of Technology
Boston, USA
harounianj@wit.edu, blanchardp2@wit.edu, marnellt@wit.edu, basnets@wit.edu

***Abstract*—The increased use of small satellites in commercial, defense, and research industries reinforces the need for efficient and reliable communication subsystems. Compact, space rated, communication subsystems present their own unique design challenges. This paper presents the design and implementation of a lower power, low form factor communication subsystem for a 1P pico-satellite, developed by a team of undergraduate students from Wentworth Institute of Technology. This effort aims to contribute to the growing field of small satellite communications by providing a robust and efficient solution.**

Keywords—Antenna, PocketQube, Dipole, Radio Frequency, Satellite, Aerospace, SWaP

I. Introduction

PocketQube satellites represent a recent advancement in the field of nanosatellites, offering a smaller and more cost-effective alternative to traditional CubeSats. The standard size for a 1U CubeSat is 10 cm³, with a weight limit of 2 kg. In contrast, a 1P PocketQube measures 5 cm³ and weighs no more than 250 grams. This scaling applies linearly with the number of units added. A significant advantage of this format is the reduced launch cost, though it comes at the expense of limited hardware capacity. The Wentworth PocketQube satellite, currently equipped with solar energy harvesters, a dipole antenna, and a magnetic attitude determination and control system (ADCS), exemplifies this balance of cost and functionality. These small satellites prove to be an effective platform for research, development, and demonstration of low Earth orbit (LEO) technologies.

LEO small satellite communication systems play a pivotal role in mission success. The obvious contributor is communication with a mission controlling ground station (GS). However, this system must be robust and equipped to handle high losses through free space, along with built in networking redundancy. It must be able to provide a reliable mode of connectivity with a ground station when overhead and optimize the small amount of time given to transmit. These 15 minute transmit windows are defined by orbital properties in a polar LEO [1].

This paper focuses on the requirements to create such a communication system. This includes antenna variations, communication link budget, component selection and finally, development and testing.

Figure 1: Render of the Wentworth PocketQube satellite [2].

II. Types of Antennas

When it comes to radio frequency transmission and reception, the choice of antenna is critical, as each type utilizes different geometries, which result in different impedances, gains, and performance characteristics. Most antenna configurations that are utilized for LEO satellite communications include patch, monopole, and dipole antennas [3]. These antennas have different radiation patterns, form factors, polarizations, and gains that all need to be heavily considered when selecting an antenna type for a communication system. A dipole antenna was selected for the Wentworth PocketQube satellite due to its omnidirectional radiation pattern, ease of implementation and stowage form factor compatibility.

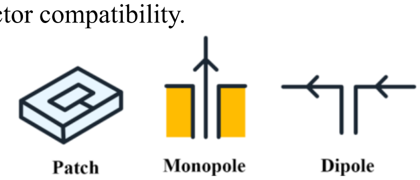

Figure 2: Common PocketQube antennae: patch, monopole and dipole [4].

III. Theoretical Link Budget

Source	***Gain/Loss***	***Unit***
Transmitter Power	+17	dBm
Transmitter Antenna Gain	+2.15	dBi
Receiver Antenna Gain	+10	dBi
Free Space Path Loss (MAX)	-153.3	dB
Antenna Pointing Loss	-1	dB
Antenna Polarization Loss	-1	dB
Atmospheric Loss	-1	dB

978-1-6654-7345-3/22/$31.00

Ionospheric Loss	-1	dB

Table 1: Theoretical Link Budget [5]

The largest loss found in the system comes from the extreme distance that the signal needs to travel. The electromagnetic signal propagates through 3D space, losing power at the rate of the distance squared. The antennas of the satellite and the GS will not point at each other with perfect accuracy, introducing more loss in the form of pointing loss. The higher the angle of error between the two antennas, the greater the pointing loss. Similarly, the electromagnetic wave polarization will also not be perfectly aligned. Both the atmospheric and ionospheric losses come from the charges suspended in our atmosphere that will attenuate our signal.

The GS will utilize the same digital transceiver as the satellite to receive the signal from LEO. The sensitivity found on the datasheet is –148 dBm [6]. Adding up the gains and losses in the communication system left a link margin of 19.85 dB. This is reinforced by amplifiers being matched at or below a 1.4 voltage standing wave ratio (VSWR). This generous margin will allow compensation for unaccounted losses such as reflections or noise in the system.

IV. Circuit Design & Development

Printed circuit boards (PCB) that contain high-speed or high-frequency signals, such as radio frequency (RF) communications require special design techniques to maintain impedance. Impedance control is an important part of design because mismatched impedances can cause signal reflections and power loss which can lead to reduced communication performance and catastrophic transmission corruption [7].

To achieve 50Ω impedance, all communications traces must be impedance matched. This involves calculating the appropriate trace width and spacing, along with using an impedance-controlled stack-up from the PCB manufacturer. This ensures that consistent copper and dielectric materials are used, and that the board is precisely manufactured. Ground vias surround the transmission line to introduce inductance that aids in cancelling out parasitic capacitances. The on-board computer has a clock signal operating at 433 MHz, which is almost exactly the RF carrier frequency. Due to the heightened concern of cross talk, an excess of electromagnetic interference (EMI) mitigation techniques were implemented. Shielding with continuous ground vias was used to create a Faraday cage around these transmission lines. The emulated Faraday cage helps protect the signals from EMI that can induce unwanted noise on the signal. An RF shield is additionally implemented on the PCB around sensitive components to assist in EMI mitigation.

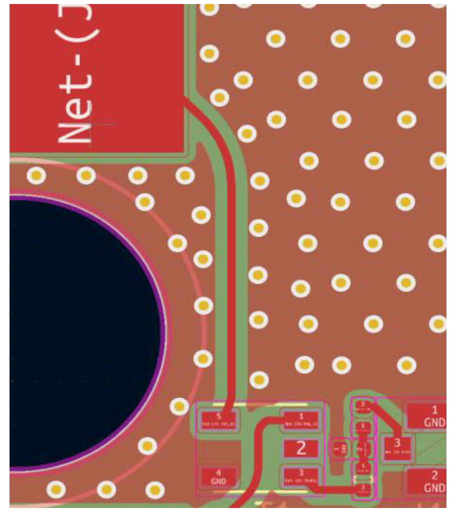

Figure 3: KiCad snippet of impedance tuned trace lined with ground vias.

This approach to impedance control helps to protect crucial communications signals so they can be transmitted efficiently and reliably while minimizing power loss and maintaining signal integrity throughout the communications system.

V. Component Selection

The small form factor presented a unique challenge while selecting RF components. To reduce the complexity of the design, adhere to form factor restrictions and reduce noise, 3.3V devices with 50Ω RF ports were selected. When selecting electronics for space applications, thermal cycling and ionizing radiation exposure are two environmental factors that must be accounted for. The thermal cycling in LEO can impose temperatures from –65° C to 125° C. Due to the low form factor and limited power budget for an active thermal management system, the Wentworth PocketQube satellite implements components of automotive grade, which include an operating thermal range of -40° C to 125° C. Radiation can induce single event upsets within components that can cause damage to on board electronics. The largest concern in a polar LEO orbit for this mission is the South Atlantic Anomaly (SAA), a low altitude section of the Van Allen belt that holds elevated levels of gamma ray ionizing radiation, which is the most damaging type to electronic components. To account for this passively with cost efficient components, firmware that implements a race to sleep design was used, with as much of the satellite powered off or in a standby state as it passes through the SAA.

A modular testing architecture was utilized in the RF front end design to isolate potential issues and expedite development time. The components selected for modular testing were the transceiver for firmware development, as well as the LNA, power amplifier, RF switch, and antenna, which will be discussed below.

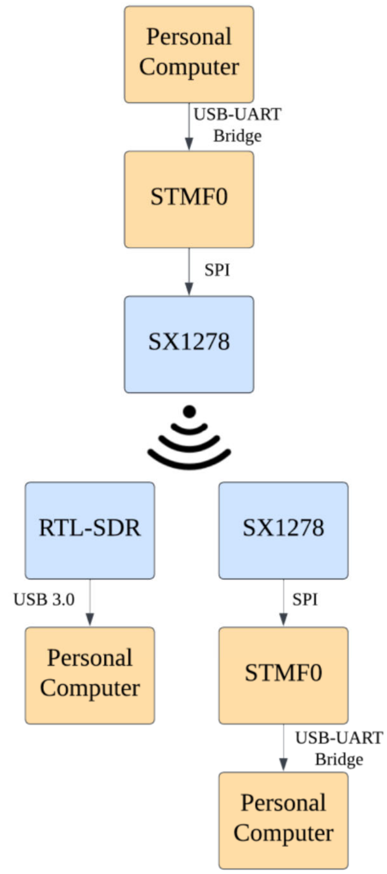

Figure 5: Setup used to test firmware on the SX1278 development board.

A) Transceiver

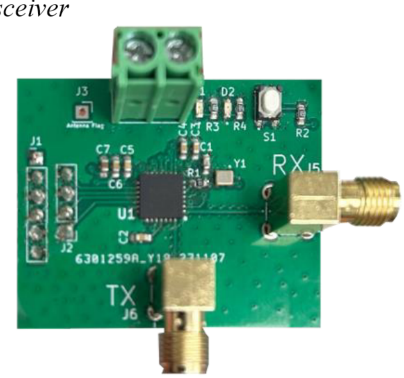

Figure 4: Development board created to test the SX1278 transceiver.

To test and observe the performance of the SX1278 transceiver and crystal oscillator, a development board was designed and fabricated. This PCB could be used alongside a microcontroller via the I2C communication protocol. This simple setup allowed the microcontroller to send commands to the SX1278, enabling its radio communication. The development board's primary purpose was to serve as a platform for preliminary testing of the SX1278's response and performance in real time. Additionally, this board ensured that the temperature-compensated crystal oscillator was accurate enough to support RF communications and was appropriate to use with the transceiver. Upon testing and observing the signal on a Software Defined Radio (SDR), the programmed frequency did not drift from the actual frequency transmitted.

Overall, the creation of this PCB was a critical step in validating the SX1278 radio module. It provided a flexible platform for early testing, ensuring that the module would meet the required performance standards before being further integrated into the satellite.

B) Power Amplifier

Due to the underwhelming parameters of the SX1278's internal power amplifier, an external amplifier was selected. This external amplifier was a Texas Instrument TRF37D73IDSGT [8]. An external amplifier introduces many benefits such as a significantly faster ramp-up time and a lower current consumption. This enhances the overall efficiency performance, providing greater power delivery to the RF signal, and a decreased noise figure when compared to the SX1278's internal amplifier. An external amplifier introduces routing and layout complexity in low SWaP applications, and the increased power level comes with a heightened thermal profile. At the operational power and frequency, the internal amplifier would take approximately 10 microseconds to ramp-up, which would significantly reduce the system's throughput. Additionally, the internal amplifier would sink 120 mA while transmitting. By contrast, the external TRF37D73IDSGT amplifier demonstrates a much shorter startup time at 600 ns and lower current consumption, making it a much more efficient option.

C) Low Noise Amplifier

The Infineon BGA420 was selected as the low noise amplifier (LNA) due to its low noise figure of 2 dBm [9] at the operating frequency, robust performance across temperature fluctuations, and low current consumption of 15 mA while receiving. The gain of the amplifier was not a primary concern because it created much more control of the transmission power of the GS than on the satellite. Instead, low noise and consistent performance were prioritized.

Initial tests showed the expected gain and acceptable input VSWR, but the output VSWR was problematic. This issue was traced to an incorrectly sized inductor. After obtaining the correct components, the goal was to achieve a VSWR of 1.5:1 or better. Properly matching the LNA and antenna will resolve these issues, preparing the module for final integration into the communication subsystem PCB.

D) RF Switch

The SKYA21001 [10] RF switch was chosen for its low insertion loss of 0.3 dB and minimal switching time, crucial for our communication subsystem. With a switching time of approximately 20 ns, it operates swiftly alongside the ramp-up times of our power amplifier and LNA, ensuring minimal disruption to signal transmission.

Integration with our digital transceiver required cascading two low-power Schmitt inverters to achieve the double-throw functionality necessary for the half-duplex communication architecture. This configuration allows the switch to alternate between transmission and reception seamlessly.

Additionally, a first order Chebyshev low-pass filter at the switch input attenuates higher frequency signals, such as those from GPS and cellular satellites, optimizing signal clarity during transmission. This reduction of high frequency noise is critical to signal integrity. These features collectively enhance the reliability and efficiency of the RF switching mechanism for the satellite's communication subsystem.

VI. Antenna Tuning Board

The baseplate's complex geometry is driven by optical constraints such as lens apertures. The dipole antenna must provide clearance for a 13mm (0.51 in) hole in between each pole, which reduces the coupling. This introduces phase shifts, length inaccuracies, and impedance mismatches that mathematical models and finite element analysis fail to characterize as accurately as testing. A PCB was created with four different dipole antenna pole layouts to be subject to impedance tuning, so the best performing variation could be implemented on the satellite.

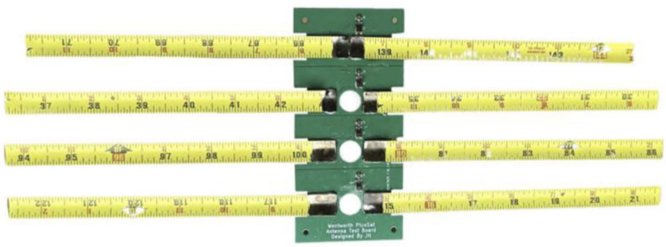

Figure 6: Antenna tuning board used for dipole development.

To create a balanced, differential signal for the dipole antenna, a balun was included in the circuit. Each variation utilizes a "T" shaped component network to tune and match the impedance of the antenna to the 50Ω transmission line. This network generally consists of a resistor, capacitor, and inductor.

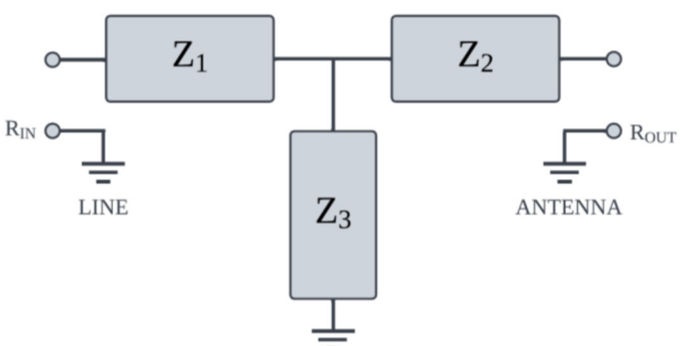

Figure 7: "T" shaped impedance tuning network [11].

A) Test Setup and Procedure

To optimally utilize this PCB to test and tune the antenna circuit, it is necessary to use a vector network analyzer. This tool measures the impedance and gain and evaluates the reflections observed when transmitting radio signals. To tune the impedance the resistor, capacitor and inductor values in the "T" shaped component network were adjusted. This changes the complex impedance and ensures all the signal's power gets transmitted through the antenna. Initially, without the matching setup, the antenna has a real impedance of 9.3Ω and a capacitive component of 22.3 pF. This would lead to most of the signal after the amplifier to be reflected, which is not ideal for long range communications. After tuning the "T" network, a 48Ω real impedance with a 2.14 nH inductive component was achieved, resulting in a –22.71 dB return loss. This is ideal because the number of reflections in the system was reduced.

Location	*Component*	*Value*
Z1	Capacitor	30pF
Z2	Capacitor	15pF
Z3	Inductor	47nH

Table 2: T-Network Component Values

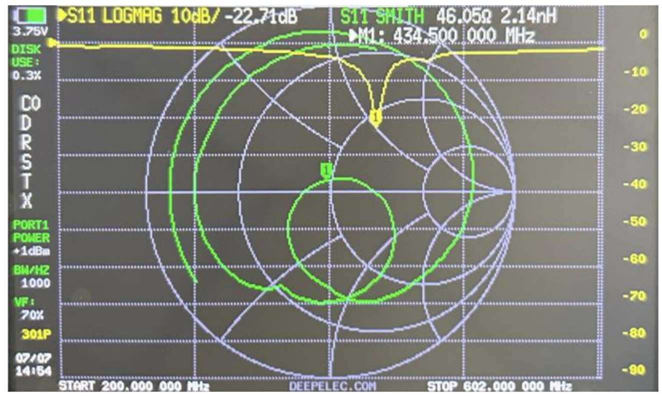

Figure 8: Virtual network analyzer output of antenna tuning board with 50Ω matched impedance.

B) Tape Measure as Dipole Medium

To maintain the 1P size dimensions of the satellite, an antenna material and geometry that would be able to deploy and expand its size after it enters its orbit was chosen. A tape measure material was used due to its steel spring-like properties and its ability to conform around the outside structure of the satellite. This allows it to be compactly stored during launch and then extended to its full length when triggered by the limit switches.

VIII. Conclusion and Future Works

The communication system for a small LEO satellite proves essential to mission completion, and eventually reaching an extended operations phase. SWaP electronics play a critical role in enabling high profile LEO missions. Small satellite technologies that continue to be developed assist all sectors of research, from the Department of Defense to academia, and to planetary sciences. The Wentworth PocketQube aims to breakthrough current small satellite technologies and uses a highly efficient satellite bus, enabling a complex mission payload. The miniaturization of RF technology and deployment of antennas in space technology proved to be integral to enhanced mission completion. Despite potential accuracies in mathematical models and FEA simulations, the data collected from testing hardware and iterations of designs proves to be the most vital component of flight readiness. From the performance of an external amplifier, to the spacing of elements on a tape measure dipole, the Wentworth PocketQube is rich in testing data and aims to breakthrough small satellite technology boundaries.

IX. Acknowledgements

The Wentworth PicoSat initiative would like to express our appreciation to Wentworth Institute of Technology for giving us the opportunity to use their facilities and resources to complete the research. Additionally, the Wentworth PicoSat initiative thanks Orion Space for assisting us by answering questions and concerns regarding the satellite and its subsystems. This research would not have been possible without their help. Finally, the Wentworth PicoSat initiative appreciates the support from Dean Ali Khabari.

References

[1] "Large Constellations of Low-Altitude Satellites: A Primer." Available: https://www.cbo.gov/system/files/2023-05/58794-satellite-primer.pdf

[2] K. M. Shanley, J. R. Rinehart, T. G. Marnell, P. R. Blanchard, M. C. Sonntag, N. Jan, D. E. Dow, F. Aveta, and S. Basnet, "Preliminary Design and Prototype for a 1P PocketQube Earth Observation Satellite," presented at the IEEE Conference, 2023.

[3] M. N. Taufique, M. F. A. Malek, M. H. M. Hamid, M. F. B. Ismail, A. Salleh, and N. E. M. S. Shah, "Antenna designs for amateur band low earth orbit (LEO) satellites - A review," International Journal of Advanced Computer Science and Applications, vol. 9, no. 9, pp. 1-8, 2018. Available: https://www.researchgate.net/publication/327644863_Antenna_Designs_for_Amateur_Band_Low_Earth_Orbit_LEO_Satellites-A_Review.

[4] E. Mikac, "What are the Most Common Types of Communication Antennae?," *CBT Nuggets Blog*, Dec. 19, 2023. [Online]. Available: https://www.cbtnuggets.com/blog/technology/networking/common-communication-antenna-types

[5] C. Jorge, R. Capela, R. Sérgio, and Cunha, "PROTOCOL OF COMMUNICATIONS FOR VORSAT SATELLITE -Link Budget," 2012. Available: https://paginas.fe.up.pt/~ee97054/Link%20Budget.pdf

[6] Semtech, "SX1278," www.semtech.com. https://www.semtech.com/products/wireless-rf/lora-connect/sx1278

[7] T. L. A. Jimenez, "UHF-VHF Cubesat Antennas Design," University of Granada, 2014.

[8] Texas Instruments, "TRF37D73IDSGT," Datasheet, Feb. 2022. [Online]. Available: https://www.ti.com/lit/ds/symlink/trf37d73.pdf?HQS=dis-dk-null-digikeymode-dsf-pf-null-wwe&ts=1722116562618

[9] I. T. AG, "BGA420 - Infineon Technologies," www.infineon.com. https://www.infineon.com/cms/en/product/rf/low-noise-amplifier-lna-ics/multi-purpose-lnas/bga420/.

[10] Skyworks, "Skyworks | Products Details SKYA21001," Skyworksinc.com, 2024. https://www.skyworksinc.com/en/Products/switches/SKYA21001.

[11] LBA Group, "T Network Diagram." Available: https://www.lbagroup.com/resources/quick-method-of-finding-t-network-values-application-note-16.